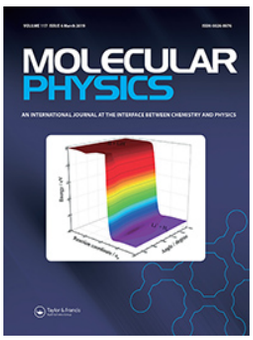

Taylor & Francis
Taylor & Francis Group

Molecular Physics

An International Journal at the Interface Between Chemistry and Physics

ISSN: 0026-8976 (Print) 1362-3028 (Online) Journal homepage: https://www.tandfonline.com/loi/tmph20

Impact of electronically excited state hydrogen bonding on luminescent covalent organic framework: a TD-DFT investigation

Manzoor Hussain, Xuedan Song, Jianzhang Zhao, Yi Luo & Ce Hao

To cite this article: Manzoor Hussain, Xuedan Song, Jianzhang Zhao, Yi Luo & Ce Hao (2019) Impact of electronically excited state hydrogen bonding on luminescent covalent organic framework: a TD-DFT investigation, Molecular Physics, 117:6, 823-830, DOI: 10.1080/00268976.2018.1543901

To link to this article: https://doi.org/10.1080/00268976.2018.1543901

MOLECULAR PHYSICS
2019, VOL. 117, NO. 6, 823–830
https://doi.org/10.1080/00268976.2018.1543901

Taylor & Francis
Taylor & Francis Group

RESEARCH ARTICLE

Impact of electronically excited state hydrogen bonding on luminescent covalent organic framework: a TD-DFT investigation

Manzoor Hussain[a,b], Xuedan Song[a], Jianzhang Zhao[a], Yi Luo[a] and Ce Hao[a]

[a]State Key Laboratory of Fine Chemicals, Dalian University of Technology, Dalian, People's Republic of China; [b]Department of Chemistry, Karakoram International University, Gilgit-Baltistan, Pakistan

ABSTRACT

The investigation of intermolecular hydrogen bonding between the luminescent polypyrene covalent organic framework and formaldehyde (PPy-COF-HCHO) was carried out with the density functional theory and time-dependent density functional theory. The strengthening of the photoexcited hydrogen bond C = O—H–C was verified via geometric structures, electronic transition energies, binding energies, UV-Vis and infrared spectra comparison in both ground state and excited state of the PPy-COF's truncated representative fragment. From the frontier molecular orbitals examination, natural population analysis, and plotted electron density difference map demonstrated that the strengthened hydrogen bond facilitated the rearrangement of electron density between H-donor and H-acceptor moieties which should account for charge transfer and ultimate fluorescence quenching. Interestingly, the energy gap between excited state and triplet state of the hydrogen-bonded complex showed the possibility of the intersystem crossing. The MOMAP programme further confirmed the quenching process because there was a lower fluorescent rate constant for the donor–acceptor PPy-COF-HCHO complex compared to free PPy-COF fragment. Results above significantly highlighted the high sensitivity of the PPy-COF towards organic analyte, i.e. the formaldehyde and can be employed as a sensor.

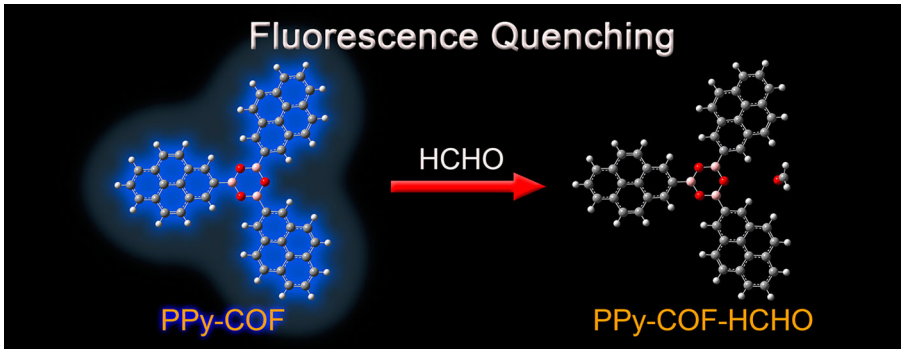

ARTICLE HISTORY
Received 28 July 2018
Accepted 28 October 2018

KEYWORDS
TD-DFT; hydrogen bonding; luminescence; MOMAP

1. Introduction

The achievement of the crystalline covalent organic framework (COF) via exclusively incorporating the light elements (H, B, C, N, and O) was the cutting-edge advancement and answer to the antiquated thinking of difficult if not impossible [1]. These light elements like carbon, boron, oxygen, and silicon; where organic units link thru strong covalent bonds: B–O, C–N, B–N, N–N, B–Si–O, alongside the extended π conjugated system [2–5]. Heretofore, the reported research regarding porous, well-defined crystalline, designable architectural features, macromolecules with covalently linked light elements, the COF is self-evident of futuristic characteristics [6]. The widened scope and COFs' value, are significantly related to the larger surface area, low mass densities, well periodic system, tunable properties, and functionality

CONTACT Xuedan Song song@dlut.edu.cn State Key Laboratory of Fine Chemicals, Dalian University of Technology, Dalian 116024, People's Republic of China

Supplemental data for this article can be accessed here. https://doi.org/10.1080/00268976.2018.1543901

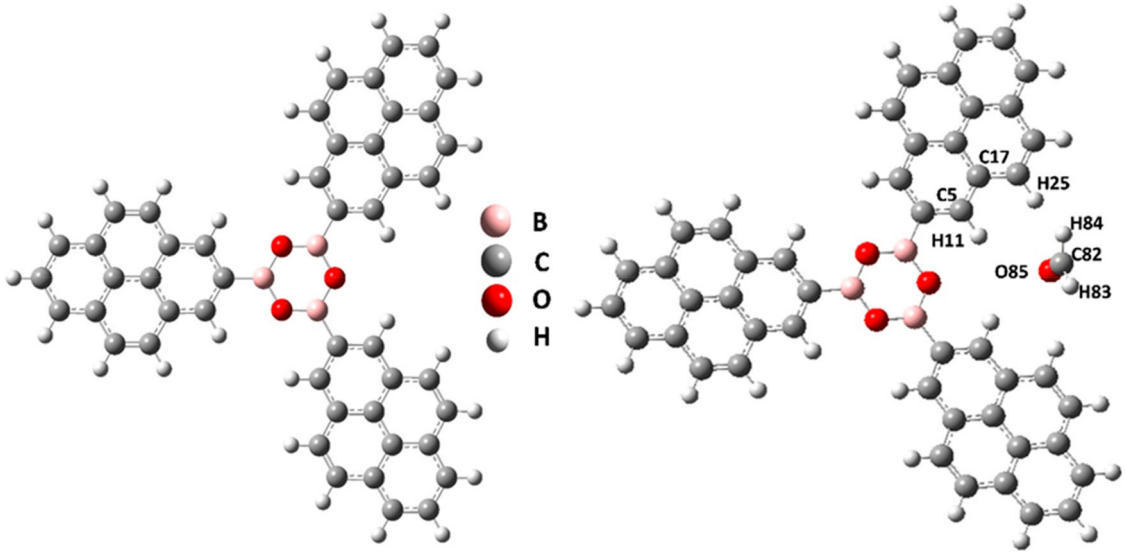

Figure 1. Optimised structures. (left) Representative COF fragment (PPy-COF); (right) Hydrogen-bonded COF complex (PPy-COF-HCHO).

as well. Resulting, COFs endow with potential applications, in particular, the gas storage, optoelectronics, catalysis, proton conduction, drug delivery, energy storage, sustainable energy, and chemosensing [7,8]. Numerous research dimensions opened after Yaghi et al. pioneering work report about the covalent organic frameworks and their synthetic routes [1,9].

Amongst COFs the 2D fluorescent covalent organic frameworks have also succeeded to bring much of researchers' attention owing to their variety of functionality as a peculiar potential for sensing [10–14]. For instance, the boronate functionals are widely employed in coupling reactions and also for the synthesis of porous crystalline frameworks on account of their low toxicity compared to transition metal catalysts. Similarly, a boroxine based functional build two, or three-dimensional porous COFs follow the process of self-condensation in diboronic acid or polyboronic acid organic skeletons. Likewise, for the current theoretical investigation, the selected COF synthesised by Wan et al. is 2D polypyrene covalent organic framework (PPy-COF) showing exciton migration, carrier transportation behaviour, photoresponsive and displays large on–off characteristics and blue luminescence property as well [15]. Furthermore, spectroscopic and other observational techniques revealed the well-ordered geometry of periodically aligned polypyrene sheets [16].

Interestingly, these types of COFs contains the function of B-O units in their main skeleton which provide an active docking site for the detection of Lewis acids-based sensitive analytes, i.e. ammonia, [3] similar to boronic acids chemosensors for biologically important species like saccharides [17]. However, these functional groups on their walls are still promising candidates for noncovalent interactions with specific gases, based on their electronegativity differences of atoms like oxygen and other electron deficient moieties. In this prospect, many experiments and theoretical simulations are focusing which provide insights into the COFs storage capacity and active functional sites for sensing applications [2,7,18]. By the abovesaid functionality and properties of PPy-COF, we at this moment expect its sensing potential for organic analytes via hydrogen bonding interaction upon photoexcitation. Therefore, the well-known indoor air pollutant formaldehyde is added to get a new understanding of hydrogen bonding dynamics. From previously reported data it is obvious that the formaldehyde has a high level of toxicity and volatility result in hazardous implication on human health particularly affects eyes and respiratory system, moreover, it is cancer causing and teratogenic as well [19–21]. Interestingly, to the best of our knowledge, this new direction of the study specifically intermolecular interaction has not been taken into consideration for covalent organic frameworks. Therefore we tended to anticipate the computational investigation regarding electronically excited hydrogen bond's strength and effect on the luminescence behaviour of the selected fragment of the PPy-COF with the newly interacted gaseous phase of the formaldehyde molecule [15].

2. The computational details

2.1. Computational model

The truncated covalent organic framework was selected as a representative fragment from the whole periodic system for further desired computations. (Figure 1 left). This fragmented PPy-COF contains three pyrene moieties

attached to boronic ester rings at vertices and eventually builds the 2D uniform layers. The terminal rings of the representative fragment were saturated with the hydrogen atoms, while formaldehyde was encapsulated in PPy-COF system with the aim of investigating the hydrogen bond dynamics in the excited (S1) state and also to unearth its impact on luminescence behaviour of the COF. Therefore the most stable isomer with the lowest energy was selected for further calculations where atomic locations, including hydrogen-bonded and other essential atoms, are appropriately represented to illustrate well in Figure 1 (right).

2.1.1. Computational methods

Quantum chemical calculations for targeted (PPy-COF) and (PPy-COF-HCHO) complex including geometry optimisation, IR spectra, UV-Vis, fluorescence emission spectra, single point energy for binding energy, the electronic transition energies as well as the NBO analysis were performed on the Gaussian 09 programme suite [22]. The employed methods were density functional theory (DFT) and time-dependent density functional theory (TDDFT) with the hybrid exchange–correlation functional B3LYP and more accepted 6-31G(d) basis sets [23,24]. Furthermore, an ADF2012 programme including the B3LYP hybrid functional and TZP basis sets was used to calculate the electronic configurations [25,26]. Similarly, the binding energy was calculated with the basis set superposition error (BSSE) correction [27,28]:

$$E_{\text{binding}} = E_{\text{PPy-COF-HCHO complex}} - E_{\text{PPy-COF}} - E_{\text{HCHO}} + E_{\text{BSSE}}$$

Additionally, the electron density difference (EDD) map was plotted by figuring the isosurfaces with the multifunctional programme the Multiwfn [29]. To give further insights into the quenching process used the TD-DFT method for the triplet (T1) state optimisation and determined the S1-T1 energy gap difference [30]. The lesser energy gap facilitates more the process of intersystem crossing (ISC), whereas the fluorescence rate constant was determined by employing MOMAP package developed by Shuai's research group [31–34]. Therefore we can predict the possible pathway of quenching phenomenon via the ISC process.

3. Results and discussion

3.1. Structure optimisation

There was consistency amongst iterated calculations and corresponding experimental data which further confirmed the reliability of a truncated representative fragment of the periodic system. For instance, the calculated optimised structure parameters and vibrational frequencies are shown in Table 1 having no imaginary modes, and also there can observe the calculated emission spectrum is in good agreement with the experimentally observed fluorescence emission [15].

Table 1. Comparison of theoretical and experimental geometry parameters and vibration frequencies for PPy-COF in the S0 state.

Bond length (Å)	Exp.[a]	DFT
B-C	1.53	1.55
B-O	1.37	1.38
bond angles (degree)		
B-C-C	121	121
O-B-C	121	121
O-B-O	119	119
dihedral angles (degree)		
O-B-C-C	180	180
O-B-C-C	0	0
vibration frequencies (cm^{-1})		
C = C stretch for fused aromatics	1588	1685
C = C vibration modes	1588, 1458	1618, 1446
B-O stretch	1380, 1339	1381, 1375
C-H out of the plane	998, 700	984, 734
fluorescence emission spectrum (nm)	410	384

[a]Reference [15].

3.2. Frontier molecular orbitals analysis and electronic configuration

Molecular orbitals (MOs) analysis can give a deep understanding of the nature of the excited state clearly [35,36]. In principle, according to the Kasha's rule, other excited states higher in energy would rapidly deactivate to the S1 vibration level. Therefore, we focused S1 and ground (S0) state because the photon emission takes place with the considerable yield from the lowest excitation state of a given multiplicity [37].

The fluorescent properties of the PPy-COF-HCHO complex were the main targeted objectives. Hence, the singlet features were taken into considerations. In this context, we described the charge transfer nature via the lowest unoccupied molecular orbital (LUMO) and the highest occupied molecular orbital (HOMO) electron density distribution. The calculated frontier molecular orbitals of PPy-COF and PPy-COF-HCHO complex were represented in Figure 2. It can see the electron density distribution of the LUMO has almost uniformly localised to polypyrene electron acceptor moieties of the COF. Whereas, the dominant localisation of electron density distribution is to one of the polypyrene moieties. While in the case of the PPy-COF-HCHO complex the electron density distribution is affected apparently due to the presence of an organic analyte, i.e. the formaldehyde in both of the LUMO and HOMO orbitals. The lowest unoccupied molecular orbital shows the majority of electron distribution towards formaldehyde, while

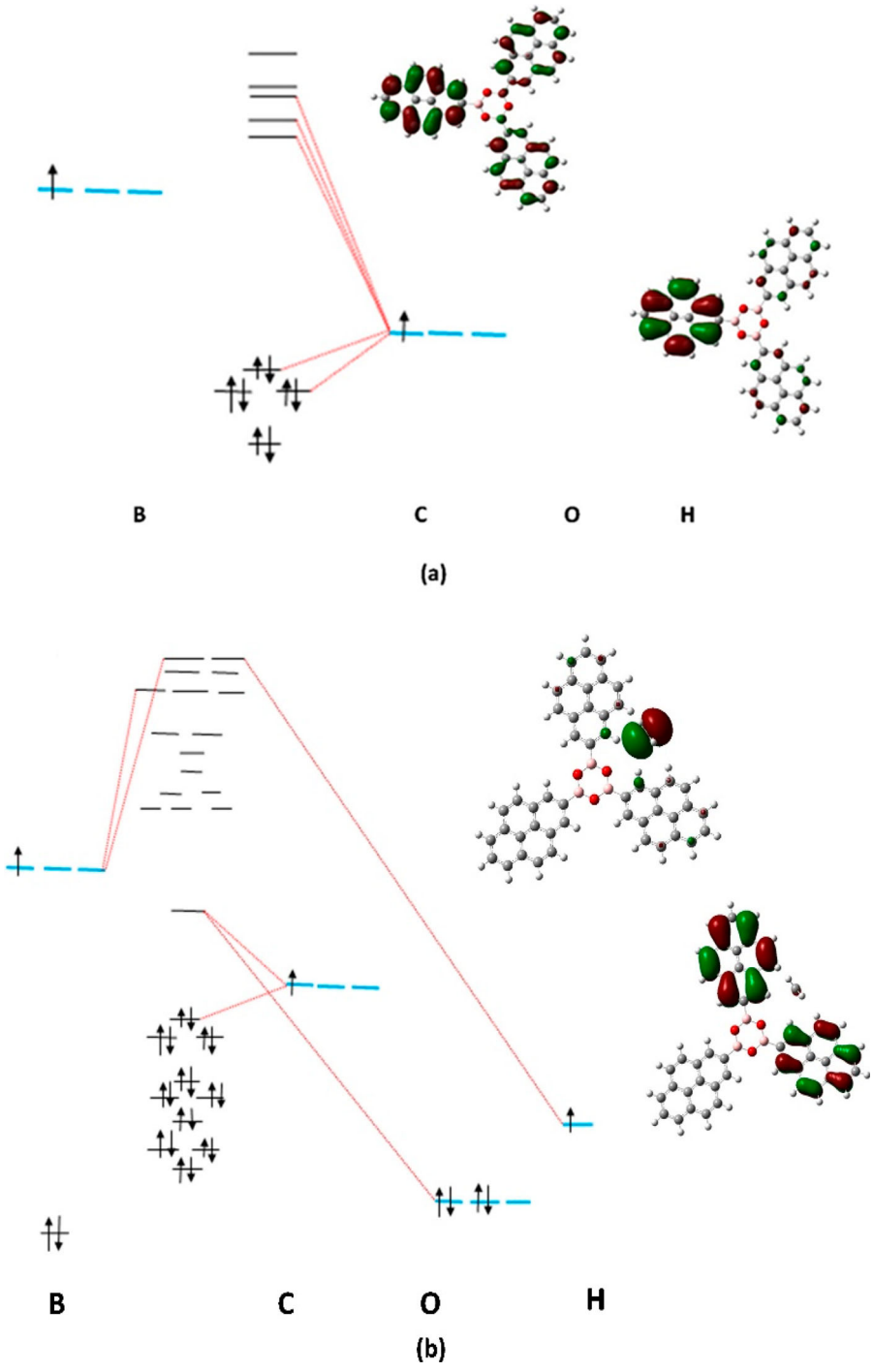

Figure 2. The Frontier MOs and the Electronic configuration for (a) PPy-COF and (b) PPy-COF-HCHO complex.

the neighbouring pyrene unit shows high-density accumulation where the hydrogen bond is dominant compared to another pyrene unit in the highest occupied molecular orbital. However, the third pyrene unit opposite to formaldehyde has not shown the density. It can easily infer the nature of noncovalent interaction based on the frontier MOs comparison, whereas it remarkably alters the charge density at LUMO of the PPy-COF. Owing to this imparting effect, it may facilitate the charge transfer process in the excitation state likely, between the PPy-COF and the formaldehyde. Consequently, the strengthened hydrogen bonding would lead a luminescence quenching. There are many previous related reports showing donor–acceptor or host–guest interactions in organic systems and charge transport variation [2,3,38,39].

Furthermore, the electronic configuration of each atomic orbital in molecular orbitals can also be deliberated to gain an understanding about the luminescence. For instance, the electronic configuration on pyrene units of PPy-COF complex is determined from the LUMO and HOMO orbitals which are comprised of P orbitals of C atoms (95.17%) and 94.83% respectively. For formaldehyde case, the LUMO of PPy-COF-HCHO complex is composed of mainly P orbitals of C atoms (59.15%), O atoms (37.31%) and H atoms (3.54%) respectively. From the analysis of the MOs above and electronic configuration, we may propose that charge transfer mechanism is due to hydrogen bond strengthening in the excited state of the H-donor H-acceptor complexation, which may ultimately bring the facilitation of fluorescence quenching phenomenon.

3.3. Natural population analysis and electron density difference map

NBO analysis provides T insight into the non-covalent interaction where charge distribution patterns can explain the transferring mechanism [40,41]. Therefore, the charge distribution on desired atoms (H25, O85) is described by natural population analysis (NPA) for PPy-COF, PPy-COF-HCHO, and HCHO in the molecular system, while their details have provided in the supporting information (pages from S19 to S27). It is very obvious that the increase in natural charge on H25 for ground and excitation states of PPy-COF-HCHO compared to PPy-COF unit is account for the strengthening of the hydrogen-bonded complex. In the ground state hydrogen-bonded complex, the natural charge of the donor H25 changes 0.008e only (from 0.237e to 0.246e). Meanwhile, for the S1 state hydrogen bond complex, the significant change 0.016e in natural charge from 0.237e to 0.253e which describes the strong hydrogen bonding.

Similarly, according to NPA, the net charge on O85 in the hydrogen-bonded complex for both S0 and S1 states decreases as compared to free formaldehyde molecule. The change in natural charge on O85 of PPy-COF-HCHO relative to the free HCHO molecule is –0.026e while –0.127e change in charge occurs in the excited state. So, both results coincide with the strengthening nature of the hydrogen bond and may result in the charge transfer possibility.

To further delineate the process of charge transfer behaviour, we analysed the distribution trend of the electron density using the Multiwfn software [29]. As seen Figure 3 the electron density difference (EDD) map shows two type of bluish colorus, i.e. aqua and lavender blue for both positive and negative parts of hydrogen-bonded complexes in the ground and excited states respectively. In Figure 3(a), it is pronounced that the positive charge on hydrogen atoms of both adjacent pyrene units to the formaldehyde is uniformly distributed showing the same nature of the hydrogen bond. While in Figure 3(b), the photoexcited strong hydrogen bond noticeably indicates the changes in electron density distribution relative to ground state hydrogen bond. Where a negative charge is shifted to the formaldehyde fragment obviously, and positive charge is increased on related hydrogen proximity. At the same time, a reasonable electron density accumulation occurs on the second pyrene moiety due to the weakening of hydrogen bonding. These results specifically the EDD map can provide a further indication of the occurrence of effective interaction and its effects as well. Thus, upon strengthening nature of hydrogen bond can give the convenient basis for conjugation interaction and ultimate quenching.

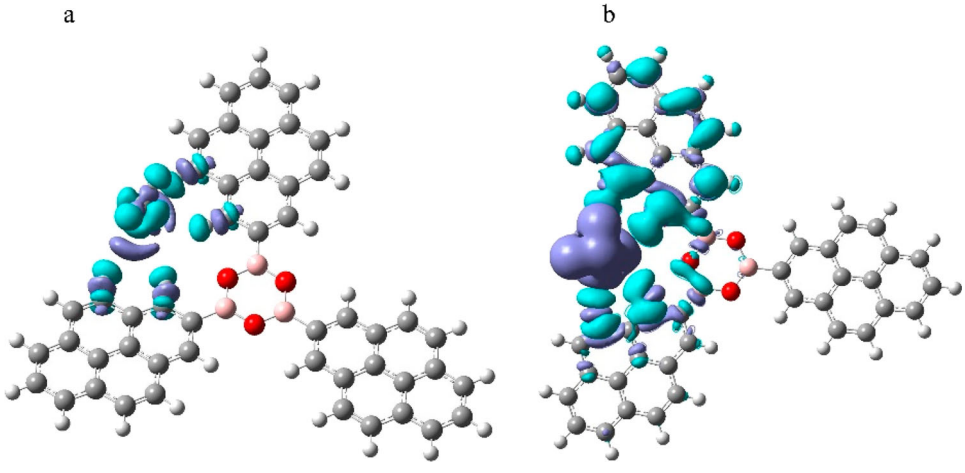

Figure 3. Aqua and lavender blue isosurfaces represent the positive and negative regions respectively in the EDD map of PPy-COF-HCHO in S0 state (a) and in S1 state (b).

Table 2. Electronic transition energies for PPy-COF and PPy-COF-HCHO complex.

Excited states	PPy-COF (eV)	PPy-COF-HCHO (eV)
S1	3.42	3.29
S2	3.42	3.29
S3	3.42	3.41
S4	3.58	3.42
S5	3.58	3.43
S6	3.58	3.55
S7	3.60	3.55
S8	3.60	3.57
S9	3.60	3.59
S10	3.65	3.59

3.4. Electronic transition energies

Zhao et al. have given a detailed summary of electronic transition energies concerning strengthened hydrogen bonding in S1 state, because hydrogen bonding can effectively influence the electronic transition energies, of the hydrogen-bonded complex [35,42,43]. This effect results in a redshift and could influence the luminescence behaviour [44]. The calculated results are in good agreement with the abovementioned theory, where the PPy-COF-HCHO complex shows lower vertical transition energies as compared to the PPy-COF fragment (Table 2).

3.5. Hydrogen bonds' properties in the electronically excited state

By using valid parameters namely hydrogen bond distance, binding energy, vibration frequencies variations, we can adequately estimate the strengthening nature of hydrogen bonding in S0 and S1 states. Hydrogen bond length can observe in Table 3 for H25—O85, where the bond length between H25—O85 is shortened from 2.76 Å in the S0 state to 2.02 Å in the S1 state with a difference of 0.74 Å with a significant change.

Table 3. Hydrogen bonding length and binding energy of PPy-COF-HCHO complex in S0 and S1 states.

Bond length (Å)	S0	S1
H25—-O85	2.76	2.02
Binding energy (kJ/mol)	−5.4	−25.0

The binding energy for the aforementioned hydrogen bond varies from −5.4 kJ/mol in the S0 state to −25.0 kJ/mol in the S1 state. As a whole, the decreasing order of binding energy is in support of the strengthened hydrogen bond dynamics in the excited state. Similarly, thru IR spectra, vibrational modes it can further examine the direct insight into the dynamics of the hydrogen bonding. The hydrogen bonds' strength can be verified from redshifted characteristic vibrational frequencies [42,45]. In this context, the influence of hydrogen bond strengthening was monitored by comparing the changes in IR spectral shifts from S0 state to S1 state. Therefore the prominent characteristic vibrational stretching frequencies of the chemical bonds in the vicinity of the hydrogen bonds have studied. Those chemical bonds are, C82 = O85, C82−H83, C82−H84, and C17−H25, with their concern peaks, can be observed from left to right in Figure 4 respectively. The stretching frequency decreased from 1829 cm^{-1} to 1559 cm^{-1} for the C82 = O85, and the second mentioned peak was about C82−H83, C82−H84 chemical bonds where the symmetric stretching frequency decreased from 2945 cm^{-1} in the S0 state to 2916 cm^{-1} in the S1 state. The same trend of redshift for asymmetric stretching frequency was noticed like 3012 cm^{-1} to −2976 cm^{-1}. Furthermore, the stretching frequency associated with the C17−H25 of fused benzene rings decreased from 3296 cm^{-1} (S0) to 3065 cm^{-1} (S1) vibration peak at the right corner in Figure 4.

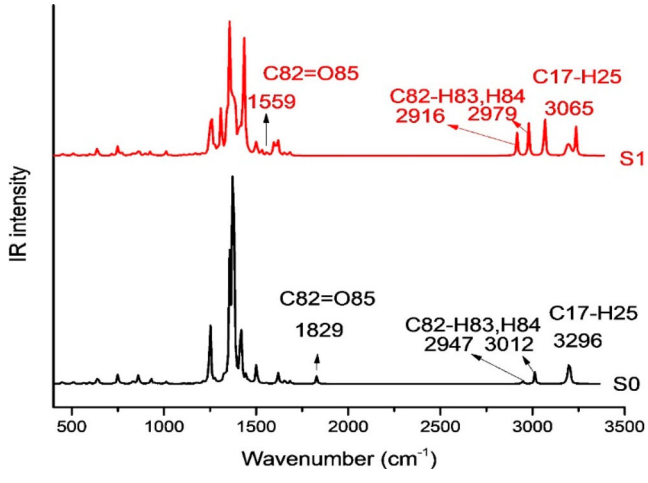

Figure 4. Stretching vibration frequency of C82 = O85, C82-H83, H84, and C17−H25 in the S0 state (black) and the S1 state (red).

All of these characteristic stretching frequencies were in red-shifted going from the S0 to S1 states. Thus these shifts also proved the hydrogen bond was markedly stronger in the S1 state compared to the S0 state.

3.6. Hydrogen bonding effect on radiative rate constant and luminescent properties

The nonradiative transition is a parallel concept to radiative transition. In other words, the lower radiative transitions cause the enhancement of nonradiative phenomenon or vice versa. For this type of transitions, the strengthened hydrogen bond in S1 state is a rationale motive based on low energy gap. In the hydrogen-bonded complex, from the S1 state to the S0 state energy gap would decrease more than that of the hydrogen-bonded free fragment ($\Delta E_{\mathrm{PPy-COF-HCHO}} > \Delta E_{\mathrm{PPy-COF}}$). The noncovalently bonded complex would show strengthened electronic coupling and thereby the maximum possibility of internal conversion (IC) from S1 state to S0 state and preferably results in the luminescence or quenching process. Another related concept is the ISC phenomenon which principally occurs when there is a smaller energy gap between electronically excited S1 and T1 states for hydrogen bonding systems. The smaller difference, the easier ISC can proceed. In the account of intersystem crossing, the luminescence would be decreased, and there might be a phosphorescence process from T1 state to S0 state vertical excitation. In PPy-COF system, S1-T1 energy gap for hydrogen bonded complex shows only 0.34 eV, while for PPy-COF fragment there is 1.21 eV (Table 4). So, this result accurately follows the energy gap law and may facilitate the ISC process. Therefore it may predict that the possible reason of the quenching mechanism is of the ISC process and PPy-COF would ultimately show the phosphorescence phenomenon.

Furthermore, in support of the phosphorescence process, a recently published article has also reported the room temperature phosphorescence property of boroxine system particularly the triphenyl-boroxine heavy-atom-free compound [46]. Similarly, our system also contains the same boroxine main skeleton with pyrene moieties. Therefore we expect the possibility of phosphorescence property in PPy-COF as well. Hence, upon the formaldehyde encapsulation, the luminescence property alters which indicating that this sensitive motif can be employed as a promising chemosensor.

Additionally, the fluorescent rate constant calculations further confirmed the impact of the encapsulated formaldehyde on luminescence behaviour due to strengthened hydrogen bond in the S1 state, where the radiative rate constant was significantly decreased for PPy-COF-HCHO complex $2.26 \times 10^3\ s^{-1}$ while the PPy-COF exhibited the $7.64 \times 10^6\ s^{-1}$, respectively.

Table 4. The calculated fluorescent rate constants of PPy-COF and PPy-COF-HCHO complex.

	PPy-COF	PPy-COF-HCHO complex
S1-T1 energy gap (eV)	1.21	0.34
Fluorescent rate constant (s^{-1})	7.64×10^6	2.26×10^3

4. Conclusion

DFT and TD-DFT theoretical calculations at the B3LYP/6-31G(d) theory level have been employed to investigate the impact of hydrogen bonding on the luminescent property of PPy-COF in the electronically excitation state. Upon evaluation of the optimised geometries including bond length, electronic transition energies, binding energies, infrared spectra, UV-Vis, and redshifts further confirmed the strengthened hydrogen bonds in the S1 state. The frontier MOs and electron configuration analysis, NPA analysis as well as the EDD map collectively represented the illustration of the strengthening hydrogen bond and impact on density distribution. Furthermore, these results provided a base for ultimate fluorescence quenching process.

Besides all, the smaller energy gap difference of the S1 state and the T1 state for PPy-COF-HCHO complex compared to PPy-COF and fluorescent rate constants calculations helped to explore the effect of the introduced molecule on the luminescent behaviour of the PPy-COF. The fluorescent rate constant for hydrogen bonded complex was determined much lower with high nanoseconds. These results revealed that the PPy-COF exhibited the high sensitivity to the formaldehyde analyte. This intriguing approach is worthy of further investigation for sensing mechanism including the selectivity and sensitivity potential of the selected COF towards small organic pollutants and other aromatic explosives to unveil their real-world applications.

Acknowledgements

We thank the National Natural Science Foundation of China (Grant Nos. 21606040 and 21677029), the Fundamental Research Funds for the Central Universities (DUT18LK26), the Supercomputing Center of Dalian University of Technology and the National Supercomputing Center in LvLiang of China.

Disclosure statement

No potential conflict of interest was reported by the authors.

Funding

We thank the National Natural Science Foundation of China (Grant Nos. 21606040 and 21677029), the Fundamental Research Funds for the Central Universities, China (DUT18LK26)

References

[1] A.P. Côté, A.I. Benin, N.W. Ockwig, M. O'Keeffe, A.J. Matzger and O.M. Yaghi, Science **310**, 1166 (2005).
[2] L. Ma, S. Wang, X. Feng and B. Wang, Chinese Chem. Lett. **27**, 1383 (2016).
[3] C.J. Doonan, D.J. Tranchemontagne, T.G. Glover, J.R. Hunt and O.M. Yaghi, Nat. Chem. **2**, 235 (2010).
[4] W. Niu, M.D. Smith and J.J. Lavigne, J. Am. Chem. Soc. **128**, 16466 (2006).
[5] L.M. Lanni, R.W. Tilford, M. Bharathy and J.J. Lavigne, J. Am. Chem. Soc. **133**, 13975 (2011).
[6] L. Zhu and Y.-B. Zhang, Molecules **22**, 1149 (2017).
[7] X. Feng, X. Ding and D. Jiang, Chem. Soc. Rev. **41**, 6010 (2012).
[8] Z. Xiang, D. Cao and L. Dai, Polym. Chem. **6**, 1896 (2015).
[9] A.L. Korich and P.M. Iovine, Dalt. Trans. **39**, 1423 (2010).
[10] R. Xue, H. Guo, T. Wang, L. Gong, Y. Wang, J. Ai, D. Huang, H. Chen and W. Yang, Anal. Methods **9**, 3737 (2017).
[11] S. Dalapati, E. Jin, M. Addicoat, T. Heine and D. Jiang, J. Am. Chem. Soc. **138**, 5797 (2016).
[12] D. Kaleeswaran, P. Vishnoi and R. Murugavel, J. Mater. Chem. C. **3**, 7159 (2015).
[13] H.L. Qian, C. Dai, C.X. Yang and X.P. Yan, ACS Appl. Mater. Interfaces **9**, 24999 (2017).
[14] Y. Wang, Z. Zhao, G. Li, Y. Yan and C. Hao, J. Mol. Model. **24** (2018).
[15] S. Wan, J. Guo, J. Kim, H. Ihee and D. Jiang, Angew. Chemie – Int. Ed. **48**, 5439 (2009).
[16] Z. Li, X. Feng, Y. Zou, Y. Zhang, H. Xia, X. Liu and Y. Mu, Chem. Commun. **50**, 13825 (2014).
[17] X. Wu, Z. Li, X.-X. Chen, J.S. Fossey, T.D. James and Y.-B. Jiang, Chem. Soc. Rev. **42**, 8032 (2013).
[18] L.A. Baldwin, J.W. Crowe, M.D. Shannon, C.P. Jaroniec and P.L. McGrier, Chem. Mater. **27**, 6169 (2015).
[19] P. Wolkoff and G.D. Nielsen, Environ. Int. **36**, 788 (2010).
[20] R. Golden, Crit. Rev. Toxicol. **41**, 672 (2011).
[21] G.D. Nielsen, S.T. Larsen and P. Wolkoff, Arch. Toxicol. **91**, 35 (2017).
[22] M.J. Frisch, G.W. Trucks, H.B. Schlegel, G.E. Scuseria, M.A. Robb, J.R. Cheeseman, G. Scalmani, V. Barone, B. Mennucci, G.A. Petersson, H. Nakatsuji, M. Caricato, X. Li, H.P. Hratchian, A.F. Izmaylov, J. Bloino, G. Zheng, J.L. Sonnenberg, M. Hada, M. Ehara, K. Toyota, R. Fukuda, J. Hasegawa, M. Ishida, T. Nakajima, Y. Honda, O. Kitao, H. Nakai, T. Vreven, J.A. Montgomery Jr, J.E. Peralta, F. Ogliaro, M. Bearpark, J.J. Heyd, E. Brothers, K.N. Kudin, V.N. Staroverov, R. Kobayashi, J. Normand,K. Raghavachari, A. Rendell, J.C. Burant, S.S. Iyengar, J. Tomasi, M. Cossi, N. Rega, J.M. Millam, M. Klene, J.E. Knox, J.B. Cross, V. Bakken, C. Adamo, J. Jaramillo, R. Gomperts, R.E. Stratmann, O. Yazyev, A.J. Austin, R. Cammi, C. Pomelli, J.W. Ochterski, R.L. Martin, K. Morokuma, V.G. Zakrzewski, G.A. Voth, P. Salvador, J.J. Dannenberg, S. Dapprich, A.D. Daniels, Ö Farkas, J.B. Foresman, J.V. Ortiz, J. Cioslowski and D.J. Fox, Gaussian, Gaussian Inc.: Wallingford, CT, (2009).
[23] A.D. Becke, J. Chem. Phys. **98**, 5648 (1993).
[24] R. Bauernschmitt and R. Ahlrichs, Chem. Phys. Lett. **256**, 454 (1996).
[25] G. Te Velde, F.M. Bickelhaupt, E.J. Baerends, C.F. Guerra, S.J.A. Van Gisebergen, J.G. Snijders and T. Ziegler, J. Comput. Chem. **22**, 931 (2001).
[26] C. Fonseca Guerra, J.G. Snijders, G. te Velde and E.J. Baerends, Theor. Chem. Accounts Theory, Comput. Model. (Theoretica Chim. Acta). **99**, 391 (1998).
[27] S.F. Boys and F. Bernardi, Mol. Phys. **19**, 553 (1970).
[28] S. Simon, M. Duran and J.J. Dannenberg, J. Chem. Phys. **105**, 11024 (1996).
[29] T. Lu and F. Chen, J. Comput. Chem. **33**, 580 (2012).
[30] M. Hussain, J. Zhao, W. Yang, F. Zhong, A. Karatay, H.G. Yaglioglu, E.A. Yildiz and M. Hayvali, J. Lumin. **192**, 211 (2017).
[31] Y. Niu, W. Li, Q. Peng, H. Geng, Y. Yi, L. Wang, G. Nan, D. Wang and Z. Shuai, Mol. Phys. **116**, 1078 (2018).
[32] Z. Shuai and Q. Peng, Natl. Sci. Rev. **4**, 224 (2016).
[33] Q. Peng, Y. Yi, Z. Shuai and J. Shao, J. Am. Chem. Soc. **129**, 9333 (2007).
[34] N. YingLi, P. Qian and S. ZhiGang, Sci. China, Ser. B Chem. **51**, 1153 (2008).
[35] D. Wu, W. Mi, M. Ji, C. Hao and J. Qiu, Spectrochim. Acta – Part A Mol. Biomol. Spectrosc. **97**, 589 (2012).
[36] Y. Liu, Y. Yang, K. Jiang, D. Shi and J. Sun, Phys. Chem. Chem. Phys. **13**, 15299 (2011).
[37] M. Kasha, Discuss. Faraday Soc. **9**, 14 (1950).
[38] S.B. Kalidindi, C. Wiktor, A. Ramakrishnan, J. Weßing, A. Schneemann, G. Van Tendeloo and R.A. Fischer, Chem. Commun. **49**, 463 (2013).
[39] D. Yang, Y. Liu, D. Shi and J. Sun, Comput. Theor. Chem. **984**, 76 (2012).
[40] Y. Zhang, Y. Duan and J. Liu, Spectrochim. Acta – Part A Mol. Biomol. Spectrosc. **171**, 305 (2017).
[41] M.M. Kabanda, V.T. Tran, K.M. Seema, R.N. Serobatse, T.J. Tsiepe, Q.T. Tran and E.E. Ebenso, Mol. Phys. **113**, 683 (2015).
[42] G.J. Zhao and K.L. Han, Acc. Chem. Res. **45**, 404 (2012).
[43] G.J. Zhao and K.L. Han, Chem. Phys. Chem. **9**, 1842 (2008).
[44] Y. Liu, J. Ding, D. Shi and J. Sun, J. Phys. Chem. A. **112**, 6244 (2008).
[45] G.J. Zhao and K.L. Han, J. Phys. Chem. A. **111**, 2469 (2007).
[46] Y. Shoji, Y. Ikabata, Q. Wang, D. Nemoto, A. Sakamoto, N. Tanaka, J. Seino, H. Nakai and T. Fukushima, J. Am. Chem. Soc. **139**, 2728 (2017).